Ultrasonics Sonochemistry 16 (2009) 50–56

Contents lists available at ScienceDirect

Ultrasonics Sonochemistry

journal homepage: www.elsevier.com/locate/ultsonch

Damage effects of protoporphyrin IX – Sonodynamic therapy on the cytoskeletal F-actin of Ehrlich ascites carcinoma cells

Xia Zhao, Quanhong Liu *, Wei Tang, Xiaobing Wang, Pan Wang, Liyan Gong, Yuan Wang

College of Life Sciences, Shaanxi Normal University, Xi'an, Shaanxi 710062, China

ARTICLE INFO

Article history:
Received 16 December 2007
Received in revised form 28 March 2008
Accepted 7 May 2008
Available online 23 May 2008

Keywords:
Sonodynamic therapy
Protoporphyrin IX
Cytoskeletal F-actin
Ehrlich ascites carcinoma cells

ABSTRACT

In this study, we report evidence of the damage effects of sonodynamic therapy (SDT) on a novel intracellular target, cytoskeletal F-actin, that has great importance for cancer treatment. Ehrlich ascites carcinoma (EAC) cells suspended in PBS were exposed to ultrasound at 1.34 MHz for up to 60 s in the presence and absence of protoporphyrin IX (PPIX). To evaluate the polymeric state and distribution of actin filaments (AF) we employed FITC-Phalloidin staining. The percentage of cells with intact AF was decreased with 10–80 μM PPIX after ultrasonic exposure, while only few cells with disturbed F-actin were observed with 80 μM PPIX alone. The fluorescence intensity of FITC-Phalloidin labeled cells was detected by flow cytometry. The morphological changes of EAC cells were observed by scanning electron microscope (SEM). The nuclei were stained with Hoechst 33258 to determine apoptosis. Cytoskeletal F-actin and cell morphological changes were dependent on the time after SDT. Some cells suffered deformations of plasma membrane as blebs that reacted positively to FITC-Phalloidin at 2 h after SDT treatment. Many of the cells showed the typically apoptotic chromatin fragmentation. The alterations were more significant 4 h later. Our results showed that cytoskeletal F-actin might represent an important target for the SDT treatment and the observed effect on F-actin and the subsequent bleb formation mainly due to apoptosis formation due to the treatment.

1. Introduction

Sonodynamic therapy (SDT) of cancer is based on preferential uptake and/or retention of a sonosensitizing drug in tumor tissues and subsequent activation of the drug by ultrasound (Us) [1–4]. Us can penetrate deeply into tissues and can be precisely focused on the target volume to effectively activate the cytotoxicity of sonosensitizers while with minimal damage to peripheral healthy tissues. This suggests that SDT is a promising new concept of modality for cancer treatment [5].

At present, SDT was mainly focused on the mechanisms of killing effects by using different ultrasound parameters and different sonosensitizers [6]. The reported mechanisms include the mechanical action, sonochemistry action, sonoporation, cavitation, apoptosis, and so on. However, the mechanism of SDT is influenced by multiple factors, the exact mechanism about SDT is still unknown, and relatively little is currently known about the cellular targets.

F-actin is one of the important cell component involved in many cell functions, such as motility, migration, division, shape, and adhesion. Literatures reported that photodynamic treatment (PDT) induced by different sensitizers affected F-actin organization in different tumor cells, and alterations of F-actin were accompanied with changes of cell shape and cell adhesion [7–9]. However, so far, the effect of SDT on cytoskeletal F-actin has not been reported. So, in this study, we report evidence of the damage effects of SDT on the novel intracellular target, cytoskeletal F-actin, to find the implication of the element in cell death and to better understand the bio-effects of SDT.

2. Materials and methods

2.1. Chemicals

Protoporphyrin IX was purchased from Sigma chemical company (St. Louis, MO, USA) and had a purity of 94% (HPLC). The chemical structure is shown in Fig. 1. FITC-labeled phalloidin and Hoechst 33258 were also obtained from the same company.

2.2. Ultrasound exposure

The experimental set-up for insonation is shown in Fig. 2. An ultrasound transducer with a diameter of 23 mm and a focal length of 43 mm was submerged in the bottom of a glass container filled

* Corresponding author. Tel.: +86 029 8531 0266.
E-mail address: lshaof@snnu.edu.cn (Q. Liu).

1350-4177/$ - see front matter © 2008 Elsevier B.V. All rights reserved.
doi:10.1016/j.ultsonch.2008.05.005

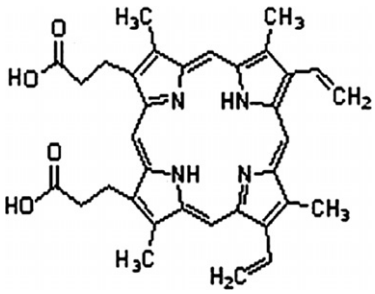

Fig. 1. Structure of Protoporphyrin IX.

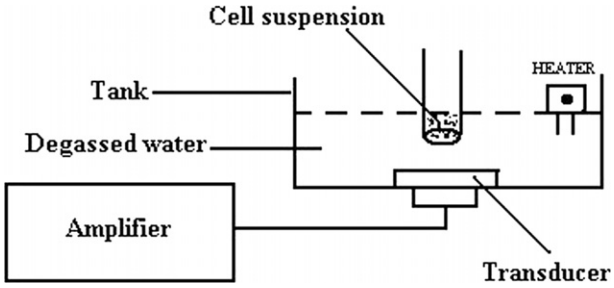

Fig. 2. Ultrasonic exposure equipment.

with cold degassed water. A polystyrene sample test tube containing 0.5 ml cell suspension was placed into the focal area of the transducer for insonation.

The ultrasound transducer was manufactured by the Institution of Applied Acoustics, Shaanxi Normal University (Xi'an, China). The same transducer was used for all the experiment, with a frequency of 1.34 MHz in a continuous wave mode, and it was used to convert the electrical power measured by the amplifier (T&C Power Conversion, Inc., Rochester, New York, USA) into acoustic power. In order to specify the intensity in the insonation experiment and have an easy and obvious understanding, we used the reading output power from the amplifier representing our spatial average ultrasound intensity in our experiment system. Otherwise, our previous investigation indicated that the real in situ intensity in the continuous wave mode could be about 60–70% of the electrical power. For all experiments, cold degassed water (4) was used as the ultrasonic coupling medium, thus reducing thermal effect caused by ultrasound irradiation. The temperature within the cell suspensions (37 °C) was checked with a thermometer and found the temperature changes was about ±1 °C, which was not likely to induce thermal damage.

2.3. Tumor cells and animals

EAC cells and ICR mice (weight: 18–22 g female) were supplied by the experimental animal center, Shaanxi Institution of Chinese Traditional Medicine (Xi'an, China). The cell line was passed weekly in the ascites of ICR mice. After 7–10 days of in vivo inoculation, the cells were harvested from the abdomen, washed 3 times by phosphate buffer solution (PBS, pH 7.4), collected by centrifugation at 2000 rpm 5 min, and then resuspended in PBS at a concentration of 3×10^6 cells/ml. Cell viability before treatment was always over 97%.

2.4. Evaluation of F-actin damage

Ultrasonically induced F-actin damage in the presence and absence of PPIX was detected immediately after SDT treatment by FITC-Phalloidin staining. EAC cells were fixed by 3.7% fresh paraformaldehyde (PFA) in PBS (pH 7.4) for 10 min at 37°C, washed in PBS, and permeabilized with 0.1% TritonX-100 in PBS. After two washes with PBS, cells were stained with 0.5 μg/ml FITC-Phalloidin for 1 h at room temperature, and then washed again in PBS. Status of F-actin polymerization was quantitated by randomly choosing at least 10 microscopic fields (40×) and counting cells in the field as either with intact or disturbed actin filaments (AF). The rate of cells with intact AF can be expressed as 'the number of cells with intact actin filaments / the total number of cells'. The data were processed by analysis of variation.

2.5. Cell survival assay

The cell viability was detected at 0, 2 and 4 h after SDT treatment by trypan blue exclusion test. A 100 μL cell suspension was taken from the sample test tube, mixed with 200 μL 0.4% trypan blue solution. Cell integrity was determined by counting the number of unstained cell on a hemocytometer glass plate using an optical microscope to estimate the number of intact viable cells and the number of nonviable cells. The count before exposure is considered 100%; while the decrease in the number of intact (viable + nonviable) cells after sonication is considered the amount of lysed cells.

2.6. Estimate of F-actin damage and morphological changes as time prolonged

2.6.1. Actin filament staining

EAC cells were placed on glass slide at 0, 2, and 4 h post treatment, fixed by 3.7% fresh paraformaldehyde (PFA) in PBS (pH 7.4) for 10 min at 37°C, washed extensively in PBS, and permeabilized with 0.1% TritonX-100 in PBS. After rinsing in PBS, cells were stained with 0.5 μg/ml FITC-Phalloidin (in PBS) for 1 h at room temperature, and then washed again in PBS. F-actin was imaged by fluorescence microscopy using a Nikon E600 microscope with 100 × oil immersion lenses. The images were captured by a CCD camera equipment with the same exposure settings.

2.6.2. Flow cytometry analysis

Cells were fixed with 3.7% fresh PFA at room temperature for 10 min after 4 h of incubation, washed with PBS, and then permeabilized with 0.1% Triton X-100. After washing three times with PBS, cells were incubated with 0.2 μg/ml FITC-Phalloidin containing 10% BSA for 1 h in dark. The cells were washed with PBS and analyzed by flow cytometry.

2.6.3. Scanning electron microscopy observation

Cells for SEM were fixed by 2.5% glutaraldehyde in 0.1 M PBS (pH 7.4) at 0, 2, and 4 h after the SDT treatment, and postfixed by 1% osmium tetroxide, then washed by PBS, dehydrated by graded alcohol, displaced, dried at the critical point, gold evaporated, and observed using a scanning electron microscope (Quanta 200, Philips-FEI company).

2.7. Detection of apoptosis

Apoptosis was observed by chromatin staining with Hoechst 33258 at 0, 2, and 4 h post SDT treatment. Cells were incubated in Hoechst 33258 at room temperature for 10 min (final concentration, 5 μg/ml), and then washed with PBS. Nuclear morphology was examined using fluorescence microscopy with standard excitation filters. The percentage of apoptotic cells was calculated, all cells from five random microscopic fields at 40× magnification were counted.

3. Results

3.1. F-actin damage

The percentage of EAC cells with intact AF in the absence of PPIX after 60 s exposure to ultrasound is shown in Fig. 3. F-actin damage did not decrease below 97% in control cells. The ultrasonically induced F-actin damage increased rapidly with ultrasound intensity above 1 W/cm^2.

The rate of EAC cells with intact F-actin in the presence of PPIX after a fixed time of insonation at an ultrasound intensity of 1 W/cm^2 is shown in Fig. 4. The ultrasonically induced F-actin damage became serious as PPIX concentration increased. PPIX enhanced the rate by more than 3 times at its concentration of 80 μM. No visible F-actin damage was observed with 80 μM PPIX alone. Additionally, the concentration of PPIX had a relatively low threshold for ultrasonically induced F-actin damage, since F-actin damage increased significantly when the PPIX concentration was greater than 20 μM.

Fig. 5 shows the rate of EAC cells with intact F-actin in the presence of PPIX for up to 60 s exposure at an ultrasonic intensity of 1 W/cm^2. The ultrasonically induced F-actin damage was enhanced as the exposure time increased, and became more significant when the exposure time was above 15 s.

3.2. Results of cell viability assay

EAC cells were exposed to ultrasound for up to 15 s at an ultrasonic intensity of 1 W/cm^2 in the presence and absence of 20 μM PPIX. The cell viability was detected at 0, 2, and 4 h. Table 1 shows the pecentage of nonviable and lysed cells in ultrasound (Us) and PPIX-SDT (Up) groups increased as time prolonged. The survival rate of cells in CT and PPIX groups changed no more than 5% after 4 h of incubation (data not shown).

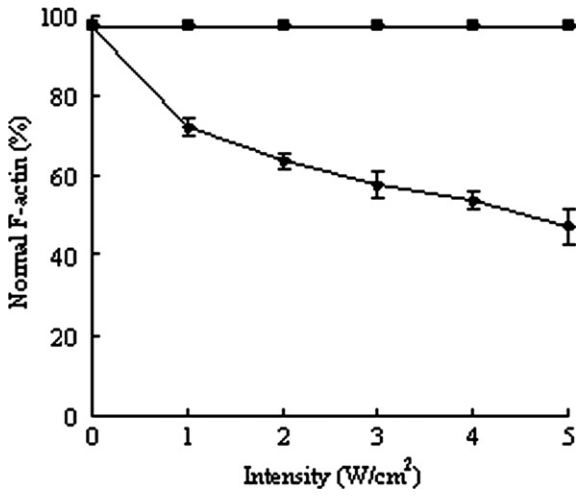

Fig. 3. Effect of 60 s ultrasonic exposure on EAC F-actin: (■) control group, (♦) ultrasound alone.

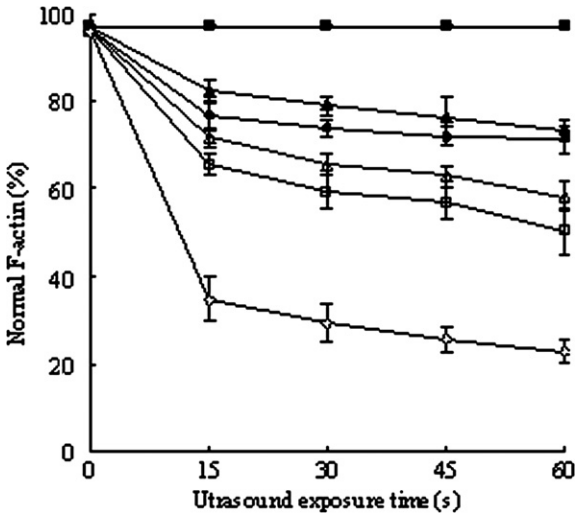

Fig. 4. Effect of ultrasound alone on EAC F-actin with and without PPIX: (■) 80 μM PPIX alone, (▲) ultrasound alone, (♦) 10 μM PPIX + ultrasound, (△) 20 μM PPIX + ultrasound, (□) 40 μM PPIX + ultrasound, (◇) 80 μM PPIX + ultrasound.

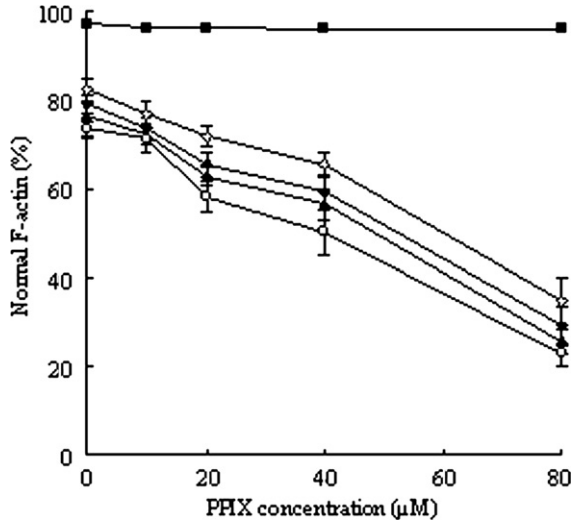

Fig. 5. EAC cells with intact F-actin after different ultrasonic exposure times in the presence of PPIX: (■) PPIX alone, (◇) 15 s, (♦) 30 s, (▲) 45 s, (○) 60 s.

3.3. Results of actin filament staining

The polymeric state and distribution of AF after 15 s exposure at an ultrasonic intensity of 1 W/cm^2 in the presence and absence of 20 μM PPIX was analyzed by using FITC-Phalloidin staining. As

Table 1
Cells viability assay

Groups	0 h		2 h		4 h	
	Nonviable (%)	Lysed (%)	Nonviable (%)	Lysed (%)	Nonviable (%)	Lysed (%)
Us	11.78 ± 1.34	1.48 ± 0.65	15.12 ± 1.76	2.17 ± 1.13	17.55 ± 2.37	3.42 ± 1.35
Up	20.47 ± 1.39	3.16 ± 1.17	24.01 ± 1.70	5.41 ± 1.52	32.01 ± 1.8	7.19 ± 1.61

The viability of EAC cells after 15 s exposure at an ultrasonic intensity of 1 W/cm^2 in the presence and absence of 20 μM PPIX was detected at 0, 2, and 4 h after treatment. The percentage of nonviable and lysed cells was given.

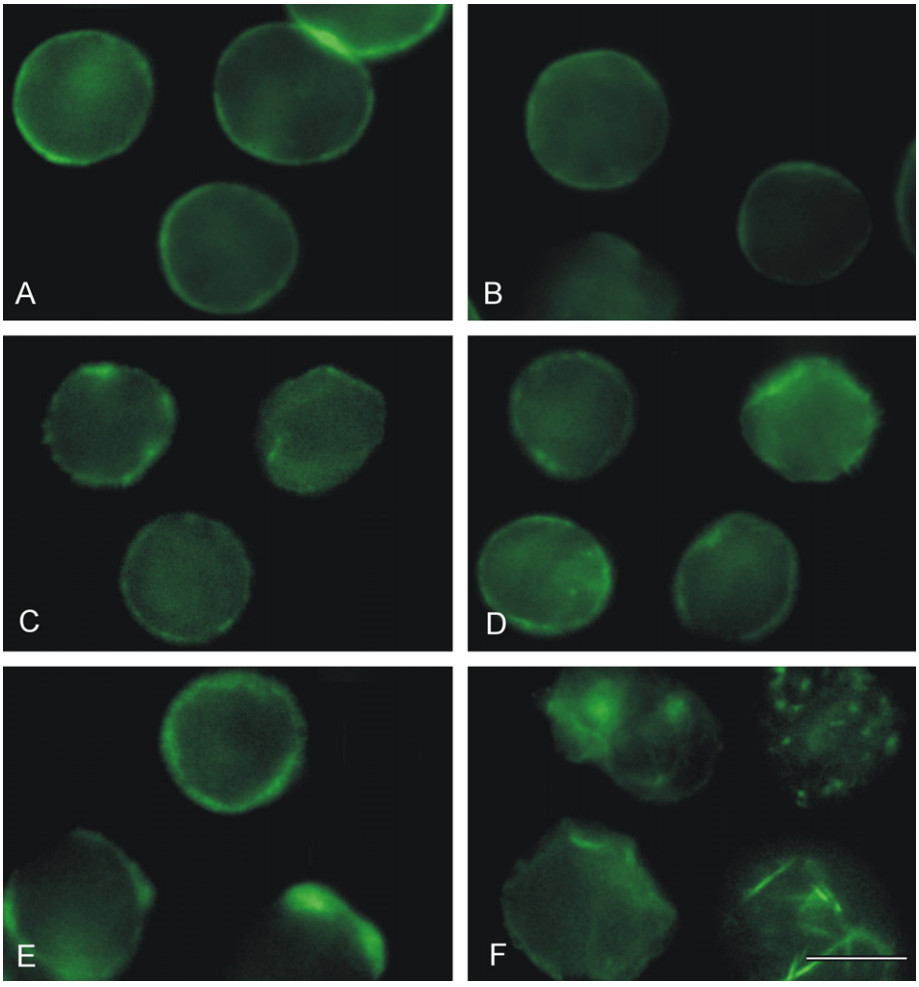

Fig. 6. Fluorescence staining of F-actin after sonodynamic treatment, labeled by FITC-Phalloidin: (A) control cells; (B, C) F-actin observed in cells at 2 and 4 h after ultrasound alone exposure. (D, E, F) F-actin observed in cells immediately after PPIX-SDT treatment or after 2 and 4 h of incubation, respectively; Scale bar: 10 μm.

shown in Fig. 6A the control cells appeared as uniformly labeled cells with a fluorescent ring on the cell surface and with no visible changes after 4 h of incubation. PPIX group cells F-actin had no obvious difference with CT group cells. The fluorescence signal of F-actin in ultrasound alone group was a part of attenuation from 2 to 4 h post-treatment (Fig. 6B and C). In the case of PPIX-SDT subjected cells AF diffused immediately after treatment (Fig. 6D). AF formed clusters and the plasma membrane lost its ring-like structure, some cells suffered deformations of plasma membrane as blebs that reacted positively to FITC-Phalloidin at 2 h after SDT treatment (Fig. 6E). The uniformly stained cells were exceptionally observed 4 h later (Fig. 6F). So, as shown in Fig. 7, the percentage of cells with disturbed actin filaments was remarkably increased in Up group as time prolonged (0 h: 28.24 ± 3.93%, 2 h: 37.75 ± 3.58%, 4 h: 51.24 ± 6.01%). It include cells with diffused and clustered F-actin (0 h: 21.08%, 2 h: 24.27%, 4 h: 28.61%) and cells with membrane blebs that filled with F-actin (0 h:4.88%, 2 h: 13.48%, 4 h: 22.63%).

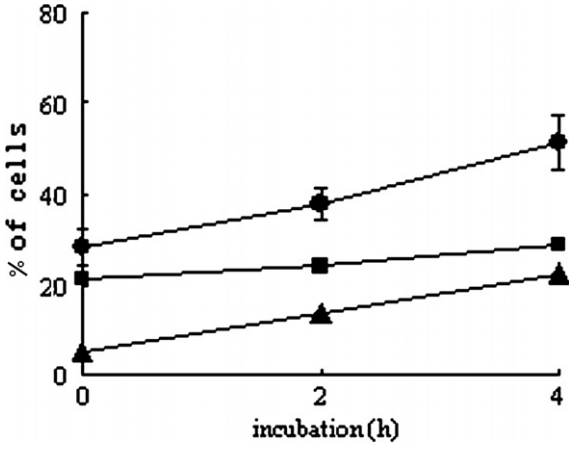

Fig. 7. Percentage of cells with disturbed F-actin in PPIX-SDT group as time prolonged: (●) the total cell with disturbed F-actin, (■) cells with diffused and clustered F-actin, (▲) cells with membrane blebs that filled with F-actin.

3.4. Results of flow cytometry

EAC cells were subjected to ultrasound at the frequency of 1.34 MHz for up to15 s in the presence and absence of 20 μM PPIX, incubated for further 4 h at 37°C and stained with FITC-Phalloidin. The fluorescence intensity of FITC-Phalloidin labeled cells was detected by flow cytometry. The percentage of cells with intact filaments was determined from the corresponding fluorescence intensity histograms. It did not decrease below 95% and 78% in control (Fig. 8A) and ultrasound alone groups (Fig. 8B), respectively. It was nearly the same with CT in PPIX alone group. The fraction of cells containing an intact cytoskeleton decreased by 39.31 ± 6% at 4 h after PPIX-SDT as shown in Fig. 8C.

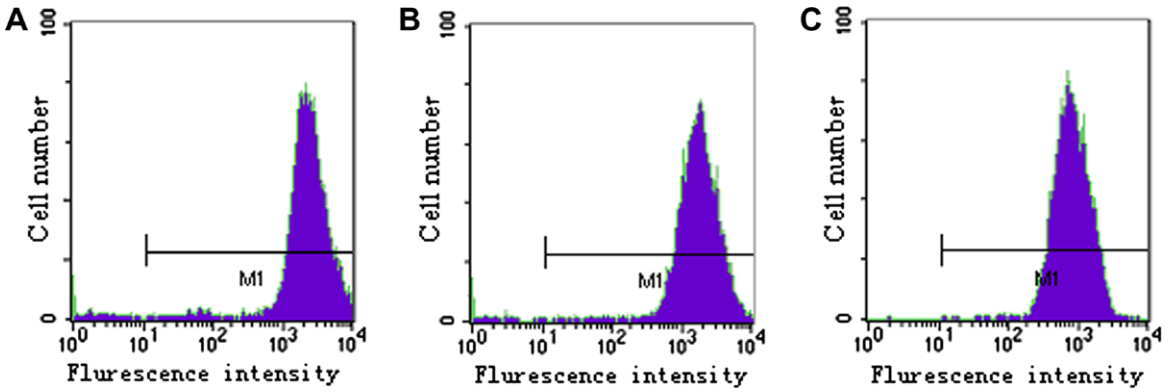

Fig. 8. Flow cytometry analysis of FITC-Phalloidin-labeled F-actin in EAC cells 4 h following PPIX-SDT. (A) Control cells; (B) irradiated with ultrasound alone; (C) cells irradiated with ultrasound plus 20 μM PPIX.

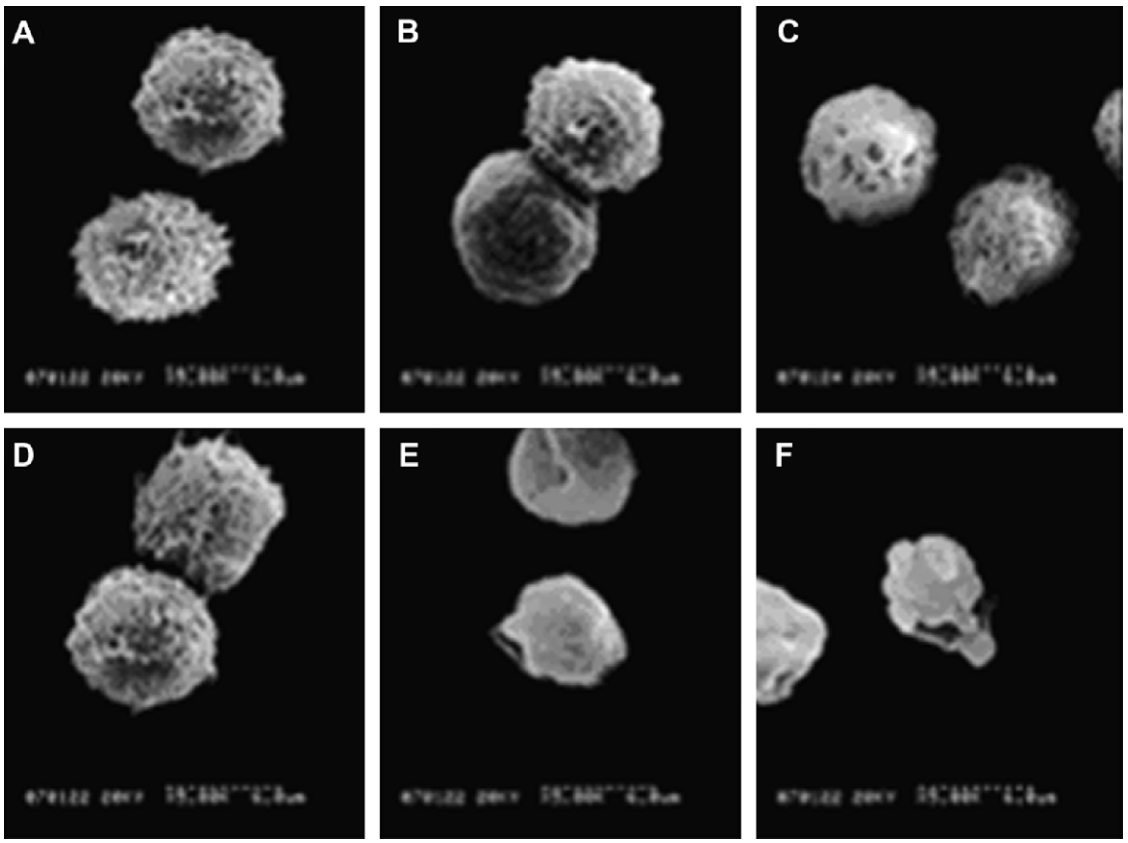

Fig. 9. SEM images of EAC cells: (A) control cell; (B, C) cells treated with ultrasound 2 and 4 h later, respectively; (D) cells 4 h after treated with 20 μM PPIX; (E, F) Cells irradiated with ultrasound plus 20 μM PPIX after 2 and 4 h of culture, respectively.

3.5. Results of scanning electron microscope observation

SEM observed the surface of EAC cells after 15 s exposure at an ultrasonic intensity of 1 W/cm^2 in the presence and absence of 20 μM PPIX. The control group showed untreated cells with numerous microvilli over the surface of the cells (Fig. 9A); PPIX alone had a slight effect on the surface of the cells, and had no obvious difference with control cells after 4 h of incubation (Fig. 9D). Cells in ultrasound alone group showed a significant decrease in the number of microvilli. The surface of many cells became relatively smooth with no obvious microvilli at 2 h (Fig. 9B). Several small craters were also seen 4 h later (Fig. 9C). Cells exposed to identical ultrasound conditions in the presence of 20 μM PPIX were seriously damaged with apparent deformation at 2 h (Fig. 9E). 4 h after the treatment, some blebs were seen in the surface of cells where the cytoplasm seemed to have extruded through the membrane boundary (Fig. 9F).

3.6. Results of Hoechst 33258 staining

Hoechst 33258 staining was used to detect the apoptosis of EAC cells after 15 s exposure at an ultrasonic intensity of 1 W/cm^2 in

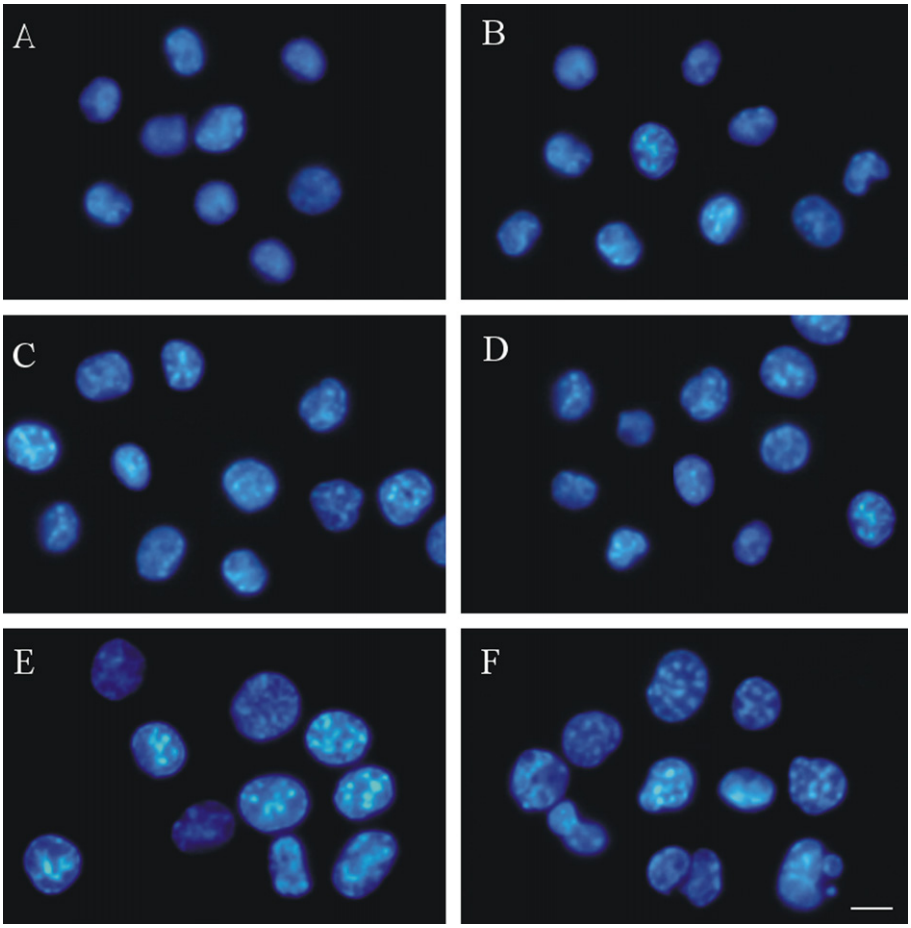

Fig. 10. Hoechst 33258 staining of EAC cells: (A) control cell; (B, C) cells treated with ultrasound 2 and 4 h later, respectively; (D, E, F) Cells irradiated with ultrasound plus 20 μM PPIX 0, 2 and 4 h later, respectively. Scale bar: 5 μm.

the presence and absence of 20 μM PPIX (Fig. 10). The control cells were uniformly blue (Fig. 10A), and cells immediately after PPIX-SDT had no visible nuclei changes (Fig. 10D). The apoptotic cells were blue and contain bright blue dots in their nuclei, representing the nuclear fragmentation. Almost 14.32% and 26.12% of the cells showed the typically apoptotic chromatin fragmentation after 2 and 4 h of incubation in Up group (Fig. 10E and F). Moreover, the cells apoptosis rate was 5.24% and 8.98% (Fig. 10B and C) at 2 and 4 h after the ultrasound alone exposure.

4. Discussion

In the present study, we investigated the damage effects of PPIX-SDT on the cytoskeletal F-actin of EAC cells. Firstly, the rate of cells with intact AF after different treatments was determined by FITC-Phalloidin staining. Significant ultrasonically induced F-actin damage was demonstrated by PPIX in our experiment. As shown in Fig. 3, the percentage of cells with intact AF decreased as the ultrasound intensity increased. The intensity threshold for ultrasonically induced F-actin damage was observed to be around 1 W/cm^2. Fig. 4 shows the significant enhancement of ultrasonically F-actin damage in the presence of PPIX. The enhancement became more significant when PPIX concentration was over 20 μM. The amount of cells with intact AF with 80 μM PPIX was about 3 times lower than with ultrasound alone under the same exposure conditions. No obvious AF damage was observed with 80 μM PPIX alone. The ultrasound exposure time also had a slight threshold for ultrasonically induced F-actin damage. This became obvious at exposure times above 15 s (Fig. 5).

So, EAC cells were subjected to ultrasonic irradiation for up to 15 s at an ultrasonic intensity of 1 W/cm^2 in the presence and absence of 20 μM PPIX. The cell viability was detected at 0, 2, and 4 h post SDT treatment, the nonviable and lysed cells were increased with time (Table 1). The polymeric state and distribution of cytoskeletal F-actin were also detected at 0, 2, and 4 h after the treatment. The results showed that F-actin presented an aberrant intracellular distribution. It was diffused and clustered after the treatment. The alterations were particularly obvious from 2 to 4 h post-treatment. Some cells suffered deformations of plasma membrane as blebs that filled with AF at 2 h after the treatment. The uniformly stained cells were exceptionally observed 4 h later (Fig. 6), and the fluorescence intensity of polymeric actin-stained cells decreased significantly due to PPIX-SDT as assessed by flow cytometry measurements (Fig. 8). Then the overall morphological changes were detected by SEM observation. Results in Fig. 9 showed that the synergistic treatment group cells were significantly influenced. The morphological changes also showed a time dependent manner, mainly including the decreasing of microvilli and the deformation of cells after SDT treatment. The surface of many cells became relatively smooth with no obvious microvilli, and many irregular blebs were seen in cell membranes in PPIX-SDT group cells from 2 to 4 h after treatment.

Membrane blebbing is one of a series of distinctive morphological events during apoptosis. It was reported to be associated with cytoplasmic and nuclear manifestations of apoptosis [10–14]. The depolymerization of F-actin is necessary for blebbing and eventual “apoptotic body” formation [15]. Cytoskeletal actin is a potential target of caspase proteases. It is partially cleaved to 15 kDa and

31 kDa fragments by activated caspases during the development of apoptosis. The actin 15 kDa fragment can induce morphologic changes [16]. Furthermore, the reorganization of microfilament network is also necessary for the formation of apoptotic bodies [15]. F-actin presents at the base of blebs [17–19] and the concentration of F-actin is correlated with bleb size [20]. In the present study, both the destruction and a reconstruction of the cytoskeletal F-actin could be seen, and F-actin presented at the base of blebs before the blebs completely formed. Feril et al. demonstrated that ultrasound could induce apoptosis [21]. Our previous work also detected that low intensity ultrasound combined with hematoporphyrin (Hp) had the apoptotic effect on EAC cells [22]. The fact that the expression of pro-apoptosis proteins (Bax, cytochrome *c*, and caspase-3) were increased with time, suggests that the apoptosis in EAC cells induced by Hp-SDT might occur through a mitochondria dependent way [23]. Recent findings indicate that mutations in actin or actin-binding proteins can influence mitochondrial pathways leading to cell death. Thus, mitochondria–actin interactions contribute to apoptosis [24]. Our recent study also found that caspase-8 might play an important role in SDT-induced apoptosis in sarcoma 180 cells in vitro [25]. Caspase 8 is an initiator caspase, stimulating the activation of several effector caspases, which, in turn, regulate the proteolytic degradation of various cellular proteins including components of the cytoskeleton. Caspase-8 and plectin are the potential mediators of the disruption of cytoskeletal F-actin [26]. So, cytoskeletal F-actin has relation with cell apoptosis regardless of the cause of apoptosis. These results suggest that the observed effect on F-actin and the subsequent bleb formation may be due to apoptosis formation due to the treatment. The increased bleb formation and loss of F-actin at 4 h further support the idea that it could have been caused by the apoptotic process induced by PPIX-SDT. Furthermore, Hoechst 33258 staining showed almost 14.32% and 26.12% of the cells underwent apoptosis after 2 and 4 h of incubation in PPIX-SDT group. The rate of cells with membrane blebs that filled with F-actin was 13.48% and 22.63% at 2 and 4 h, which was in accordance with the results of Hoechst 33258 staining.

Additionally, changes of several cytoskeleton organizing proteins [9] due to SDT treatment may play important roles in AF appeared as clusters (Fig. 6E and F) in the treated cells contrary to uniformly stained control cells.

In summary, the results indicate that F-actin is an important subcellular target for the SDT treatment in EAC cells, and the changes of cytoskeletal F-actin have some correlations with cell apoptosis. The damage to the cytoskeletal F-actin induced by the SDT of cancer has not been studied in detail compared with other subcellular structures. However, the result presented here, as well as previous data reported by other workers, strongly suggest that the effects of SDT on the cytoskeletal F-actin could also contribute to cellular inactivation. Taking into consideration of the important role of cytoskeletal components in cancer cells, further studies of the effect of SDT on cytoskeletal elements, not only F-actin, should be performed.

Acknowledgments

This work was supported by the National Natural Science Foundation of China (Grant Nos. 39870240 and 30270383) and the Excellent Doctor Innovation Project of Shaanxi Normal University.

References

[1] S. Umemura, N. Yumita, R. Nishigaki, et al., Mechanism of cell damage by ultrasound in combination with hematoporphyrin, Jpn. J. Cancer Res. 81 (1990) 962–966.
[2] K. Umemura, N. Yumita, R. Nishigaki, et al., Sonodynamically induced antitumor effect of pheophorbide a, Cancer Lett. 102 (1996) 151–157.
[3] N. Yumita, R. Nishigaki, K. Umemura, et al., Hematoporphyrin as a sensitizer of cell damaging effect of ultrasound, Jpn. J. Cancer Res. 80 (1989) 219–222.
[4] N. Yumita, R. Nishigaki, K. Umemura, et al., Synergetic effect of ultrasound and hematoporphyrin on sarcoma 180, Jpn. J. Cancer Res. 81 (1990) 304–308.
[5] T. Yu, Z. Wang, T.J. Mason, A review of research into the uses of low level ultrasound in cancer therapy, Ultrason. Sonochem. 11 (2004) 95–103.
[6] Q.H. Liu, X. Wang, P. Wang, et al., Sonodynamic effects of protoporphyrin IX disodium salt on isolated sarcoma 180 cells, Ultrasonics 45 (2006) 56–60.
[7] A. Juarranz, J. Espada, J.C. Stockert, et al., Photodamage induced by Zinc(II)-phthalocyanine to microtubules, actin, alpha-actinin and keratin of HeLa cells, Photochem. Photobiol. 73 (2001) 283–289.
[8] A. Uzdensky, E. Kolpakova, A. Juzeniene, et al., The effect of sub-lethal ALA-PDT on the cytoskeleton and adhesion of cultured human cancer cells, Biochim. Biophys. Acta 1722 (2005) 43–50.
[9] M. Pluskalová, G. Peslová, D. Grebenová, et al., Photodynamic treatment (ALA-PDT) suppresses the expression of the oncogenic Bcr-Abl kinase and affects the cytoskeleton organization in K562 cells, J. Photochem. Photobiol., B 83 (2006) 205–212.
[10] J. Huot, F. Houle, S. Rousseau, et al., SAPK2/p38-dependent F-actin reorganization regulates early membrane blebbing during stress-induced apoptosis, J. Cell Biol. 143 (1998) 1361–1373.
[11] N.J. McCarthy, M.K. Whyte, C.S. Gilbert, et al., Inhibition of Ced-3/ICE-related proteases does not prevent cell death induced by oncogenes, DNA damage, or the Bcl-2 homologue Bak, J. Cell Biol. 136 (1997) 215–227.
[12] J.N. Lavoie, C. Champagne, M.C. Gingras, et al., Adenovirus E4 open reading frame 4-induced apoptosis involves dysregulation of Src family kinases, J. Cell Biol. 150 (2000) 1037–1056.
[13] M.L. Coleman, E.A. Sahai, M. Yeo, et al., Membrane blebbing during apoptosis results from caspase-mediated activation of ROCK I, Nat. Cell Biol. 3 (2001) 339–345.
[14] M. Sebbagh, C. Renvoizé, J. Hamelin, et al., Caspase-3-mediated cleavage of ROCK I induces MLC phosphorylation and apoptotic membrane blebbing, Nat. Cell Biol. 3 (2001) 346–352.
[15] M.G. Levee, M.I. Dabrowska, J.L. Lelli Jr., et al., Actin polymerization and depolymerization during apoptosis in HL-60 cells, Am J Physiol. 271 (1996) C1981–1992.
[16] T. Mashima, M. Naito, T. Tsuruo, Caspase-mediated cleavage of cytoskeletal actin plays a positive role in the process of morphological apoptosis, Oncogene 18 (1999) 2423–2430.
[17] S.M. Laster, J.M. Mackenzie Jr., Bleb formation and F-actin distribution during mitosis and tumor necrosis factor-induced apoptosis, Microsc. Res. Tech. 34 (1996) 272–280.
[18] F. Pitzer, A. Dantes, T. Fuchs, et al., Removal of proteosomes from the nucleus and their accumulation in apoptotic blebs during programmed cell death, FEBS Lett. 394 (1996) 47–50.
[19] G.S. Vemuri, J. Zhang, R. Huang, et al., Thrombin stimulates wortmannin-inhibitable phosphoinositide 3-kinase and membrane blebbing in CHRF-288 cells, J. Biochem. 314 (1996) 805–810.
[20] C.C. Cunningham, Actin polymerization and intracellular solvent flow in cell surface blebbing, J. Cell Biol. 129 (1995) 1589–1599.
[21] L.B. Feril Jr., T. Kondo, Z.G. Cui, et al., Apoptosis induced by the sonomechanical effects of low intensity pulsed ultrasound in a human leukemia cell line, Cancer Lett. 221 (2005) 145–152.
[22] Q.H. Liu, Pan Wang, Meng Li, et al., Apoptosis of Ehrlich ascites tumor cells by sonochemical activated hematoporphyrin, Acta Zool. Sinica 49 (2003) 620–628.
[23] Q.H. Liu, S.Y. Liu, H. Qi, et al., Preliminary study on the mechanism of apoptosis in Ehrlich ascites tumor cells by sonochemical-activated hematoporphyri, Acta Zool. Sinica 51 (2005) 1073–1079.
[24] I.R. Boldogh, L.A. Pon, Interactions of mitochondria with the actin cytoskeleton, Biochim. Biophys. Acta 1763 (2006) 450–462.
[25] W. Tang, Q. Liu, X. Wang, et al., Involvement of caspase 8 in apoptosis induced by ultrasound-activated hematoporphyrin in sarcoma 180 cells in vitro, J Ultrasound Med. 27 (2008) 645–656.
[26] M. Beil, J. Leser, M.P. Lutz, et al., Caspase 8-mediated cleavage of plectin precedes F-actin breakdown in acinar cells during pancreatitis, Am J Physiol Gastrointest Liver Physiol. 282 (2002) G450–G460.